

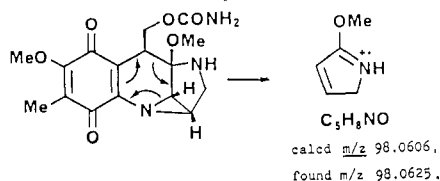
moiety, but **1** showed the R band of 525 nm (in MeOH).⁸ In contrast with the complex carbonyl stretching region of **1**'s IR (KBr) the simplified carbonyl absorptions⁹ of **2** also implied the transformation of the quinone skeleton.

The inspection of ¹H and ¹³C NMR spectra of **2** revealed that the skeleton was extremely close to **1** except for the fact that the quinone of **1** was converted to 2-hexene-1,4-dione moiety in **2**. The relative configuration between the appeared methine proton at C-8a and the carbamoyloxymethyl was determined to be cis by the presence of significant NOE.¹⁰ The C-4a (δ 87.5 in CDCl₃) was suggestive of the dihetero-atom-substituted sp³ carbon in view of the chemical shift. Thus the full structure was led by the reasonable connection between the C-4a with the nitrogen of the aziridine considering the molecular formula.¹¹

The discovery of **2** prompted us to search for a new tetracyclic isomer of **1**, because intramolecular retro-Michael reactions of **2** may afford both **1** and **3**. Our efforts were directed toward investigating the culture broth, and we succeeded in isolating the expected **3**.⁴

Isomitomycin A (**3**), obtained as yellowish orange needles from CHCl₃ (mp 78–80 °C, [α]_D²³ –273 °C (c 0.17, CHCl₃), on TLC silica gel was converted, in part, to **1** and **2** in several hours. The molecular formula, C₁₆H₁₉N₃O₆, was determined in the same way as **2**.¹³ The mass spectrum of **3**¹⁴ was partly different from that of **1** and showed the characteristic fragment, *m/z* 98 (base peak; described later), which was not found in **1**. The electronic spectrum¹⁵ showed the presence of a quinone. IR (KBr)¹⁶ showed a band ascribable to a carbamoyl carbonyl (1721 cm^{–1}).

The analysis of ¹H and ¹³C NMR spectra¹⁰ verified the partial structure resembling C-4a through C-10 in **1** and another right wing skeletal connection consisting of a secondary amine, a methylene, and an aziridine. The plane structure of **3** was led by connecting N-7b with C-7a and C-2a with C-3 and N-2, respectively, on the basis of LSPD experiments.¹⁷ This novel tetracyclic ring system was also supported by the fragment ion (*m/z* 98) in EI-MS, which could be interpreted as an intermediate generated by the retro-Diels–Alder reaction in **3**. The stereochemistry was unambiguously determined by the chemical property; **3** was able to be easily transformed to **1** via **2**.



In the study of structure elucidation of **3** it became of interest to examine whether **1** in itself could be transformed to **2** or **3** in a solution or not. In practice, both transformations of **1** to **2** and

1 to **3** via **2** were confirmed by HPLC in a protic solvent. Thus the absolute structures of both **2** and **3** were uniquely determined to have a relationship with that of **1**.¹⁸ They were equilibrated in MeOH at room temperature within 3 days, and the equilibrium trended to **1**.¹⁹ In an aprotic solvent, they were stable in several days. However, we found some Lewis acids, e.g., triisopropoxy-aluminum, accelerated the rearrangement reaction even in an aprotic solvent.

A remarkable structural feature of **2** is the unprecedented pentacyclic ring system. Another conspicuous characteristic of **2** is that this new ring system would be exchangeable to the mitomycin skeleton and the novel 2,7b-diazabenzocycloprop[cd]indene-4,7-dione skeleton of **3** through an intramolecular retro-Michael reaction. The structures of **2** and **3** present a new and promising pathway for the total syntheses of mitomycins²⁰ and mitomycin analogues which would be clinically more valuable than mitomycin C.¹ The study of a new analogue by the use of **2** and **3** is under way.

Acknowledgment. We are grateful to Dr. M. Kasai for his help in the preparation of this paper.

Supplementary Material Available: The procedures of chromatographic separations for **2** and **3**; listing of ¹H and ¹³C NMR data for **1**, **2**, and **3**; and listing of the equilibrium ratio of **1**, **2**, and **3** in various solvents (5 pages). Ordering information is given on any current masthead page.

(18) (a) Shirahata, K.; Hirayama, N. *J. Am. Chem. Soc.* **1983**, *105*, 1799. (b) Hirayama, N. *Acta Crystallogr. Sect. A: Found Crystallogr.* **1984**, *A40*, C-70. (c) This conclusion was independently verified on the basis of circular dichroic measurements. Verdine, G. L.; Nakanishi, K. *J. Chem. Soc., Chem. Commun.* **1985**, 1093.

(19) The table of the equilibrium ratio in some solvents is given in the Supplementary Material.

(20) During the processing of this manuscript, Fukuyama reported synthetic approaches toward mitomycins via isomitomycin A (**3**). Fukuyama T.; Yang, L. *Tetrahedron Lett.* **1986**, *27*, 6299.

Temperature-Dependent Geometric Isomerization Versus Fragmentation of 1,2-Dideuteriocyclobutane

David K. Lewis,*† David A. Glenar,‡ Bansi L. Kalra,§
John E. Baldwin,*[⊥] and Steven J. Cianciosi[⊥]

Departments of Chemistry and Physics
Colgate University, Hamilton, New York 13346
Department of Chemistry, Syracuse University
Syracuse, New York 13244

Received April 3, 1987

Fresh insights on the 1,4-diradical tetramethylene^{1–4} generated thermally from tetrahydropyridazine (TP) and from cyclobutane (CB) have been gained through studies of stereospecifically deuteriated substrates.^{5–9} At 380–420 °C, tetramethylene fragments to ethene about twice as fast as it closes to form CB; the two ends of the diradical appear to be stereochemically independent, with rotations about C–C bonds much more rapid than

(8) Uzu, K.; Harada, U.; Wakaki, S. *Agr. Biol. Chem.* **1964**, *28*, 388.

(9) IR spectra (KBr): **1** (1500–1800 cm^{–1}) 1727, 1701, 1665, 1641, 1627, 1584, 1568 cm^{–1}; **2** 3500, 3370, 2970, 2940, 1737, 1696, 1658, 1598, 1333, 1303, 1235, 1134, 1063, 1045, 955 cm^{–1}.

(10) ¹H and ¹³C NMR data for **2** and **3** are given in the Supplementary Material.

(11) Due to the absence of certain results in LSPD experiments in CDCl₃ and Py-*d*₅ we were unable to connect C-4a with the nitrogen of the aziridine at the beginning. The answer for this problem was given by the concurrent of X-ray crystallography for the relative configuration.¹² Later the C-4a was proven to be located in the neighborhood of H-1 by LSPD in DMSO-*d*₆.¹⁰

(12) This study was made independently. Hirayama, N.; Shirahata, K., *Acta Crystallogr., Sect. B*, to be published.

(13) Anal. Calcd for C₁₆H₁₉N₃O₆: C, 55.01; H, 5.48; N, 12.03. Found: C, 55.16; H, 5.55; N, 11.74. HRMS calcd for C₁₆H₁₉N₃O₆ *m/z* 349.1274, found *m/z* 349.1237.

(14) Mass fragments of **3**: *m/z* 349 (M⁺), 288, 275, 259, and 98.

(15) The electronic spectrum of **3**: λ_{max}^{MeOH} 294 nm, ε 5200, 410 nm, ε 340. Strong end absorption was observed to 240 nm.

(16) IR spectrum (KBr): **3** 3500, 3440, 3360, 2950, 2860, 1721, 1701, 1694, 1642, 1595, 1334, 1307, 1228, 1216, 1081.

(17) The LSPD experiment in CDCl₃ provided unambiguous connectivity for the C-7a with the nitrogen of the aziridine; that is, an irradiation at H-7d (δ 3.17) or H-7c (δ 3.57) made the spectral wave form change more markedly on C-7a (δ 148.6) than that at H-1 (δ 3.33). The connection between the C-2a and the C-7d was supported by the LSPD experiment in CDCl₃; that is, an irradiation at H-7d (δ 3.17) enhanced the resonance at C-2a (δ 92.4).

* Department of Chemistry, Colgate.

† Department of Physics, Colgate; present address: Code 693, NASA Goddard Space Flight Center, Greenbelt, MD 20771.

‡ Department of Chemistry, Colgate; permanent address: Department of Chemistry, Hollins College, Roanoke, VA 24020.

[⊥] Syracuse.

(1) Hoffmann, R.; Swaminathan, S.; Odell, B. G.; Gleiter, R. *J. Am. Chem. Soc.* **1970**, *92*, 7091–7097.

(2) Doering, W. v. E. *Proc. Natl. Acad. Sci. U.S.A.* **1981**, *78*, 5279–5283.

(3) Schaumann, E.; Ketcham, R. *Angew. Chem.* **1982**, *21*, 225–314.

(4) Dervan, P. B.; Dougherty, D. A. In *Diradicals*; Borden, W. T., Ed.; Academic Press: New York, 1982; pp 107–149.

Table I. Ratios of Products from Shock Tube Heating of *cis*-1,2-Cyclobutane-*d*₂^a and Ratios of Rate Constants^b

T (K)	ethenes (%)	1/2	3/4	$k_{\text{fr}}/k_{\text{g}}^b$	$k_{\text{fr}}/k_{\text{fi}}^b$	$\Delta\Delta G^\ddagger^c$
693				4.1 ± 0.3^d	$\approx 1.0^d$	1.0 ± 0.1
980	2		2.5 ± 1.0		2.5 ± 1.0	
1048	24	12 ± 3	1.5 ± 0.1	3.3 ± 0.9	1.5 ± 0.1	0.6 ± 0.6
1130	75	4.9 ± 1.0	1.4 ± 0.1	6.8 ± 1.4	1.5 ± 0.1	2.2 ± 0.5

^a C₄H₆D₂ (2–4%) in Ar, pressure during reaction ≈ 2 atm. ^b As defined in Scheme I. ^c Deduced difference, kcal/mol, between barriers to fragmentation and ring closure of diradical. ^d Reference 8, static reactor.

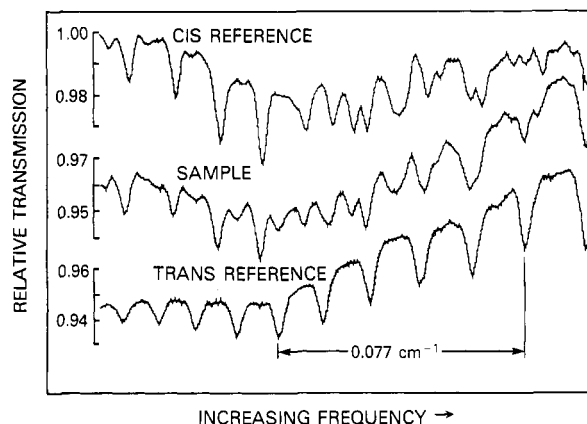


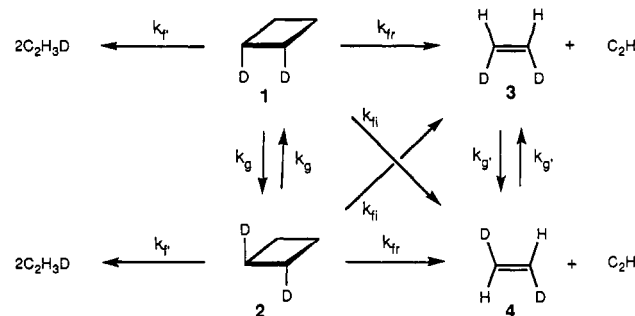
Figure 1. TDL spectra for calibration samples (*cis*, 0.93 Torr, 90-cm path; *trans*, 0.95 Torr, 30-cm path) and for cyclobutane-1,2-*d*₂ products of shock tube experiment at 1130 K (0.95 Torr, 90-cm path).

either recombination or dissociation.^{5–9}

Theoretical models have suggested that singlet tetramethylene may have only a shallow or no potential energy minimum.^{1,10,11} It may, however, be relatively stable on the free-energy surface:¹⁰ entropies of transition-state structures leading to dissociation or CB formation should be lower than for the diradical and could be different. Experimental measurement of the variation with temperature of the $k(\text{fragmentation})/k(\text{isomerization})$ ratio and the extent of retention of reactant stereochemistry in the ethene product would provide direct information about the relative temperature dependence of ΔG^\ddagger for the competing exit channels.

That experiment has now been performed, by using shock-tube kinetic techniques to study the competitive fragmentation and geometric isomerization reactions shown by *cis*-CB-1,2-*d*₂ over a significant range of temperature and tunable diode laser infrared spectroscopy to determine the stereochemistry of the CB-1,2-*d*₂ and ethene-1,2-*d*₂ product samples.

Authentic *cis* and *trans* samples of CB-1,2-*d*₂ (**1** and **2**) and ethene-1,2-*d*₂ (**3** and **4**) as well as of CB-*d*₁, ethene-*d*₁, and CB-1,1-*d*₂ were prepared following routes detailed in the literature.^{5,6,12–14} The single-pulse shock tube in which samples of **1** were heated to 980–1130 K and the TDL/computer instrumentation have been described elsewhere.^{15–18} Fragmentation to

Scheme I

ethene was measured by vapor-phase chromatography, and geometric isomerization of **1** to **2** was monitored with the TDL spectrometer, as was the ratio of **3** to **4** in product gas samples.

Figure 1 shows scans of infrared absorption by reference samples of **1** and **2**, and by CB products from a kinetic run at 1130 K, over a 0.16-cm^{−1} spectral range at 1298 cm^{−1}. Although the vibrational frequencies of the *cis* and *trans* isomers are essentially degenerate in this region,¹⁹ the different stereochemical dispositions of deuterium labels separate the *v*,*r* transitions. Curve fitting over the many absorption features allowed numerous measurements of *cis*/*trans* abundance from each sample; these were then averaged. Absorption features of **3** and **4** at 912 and 991 cm^{−1} were several hundred times as intense at comparable pressures and completely resolved. TDL analyses showed no formation of CB-1,1-*d*₂. Mass spectrometric analysis showed no CB-*d*₃ products at 980 or 1048 K, and only possible traces at 1130 K. Gas chromatography indicated that the reaction was extremely clean at 980 and 1048 K, but traces of isomeric butenes, butadiene, and smaller compounds were produced at 1130 K, suggesting some radical-induced decomposition of cyclobutane at that temperature.

The measured product ratios (Table I) were modeled on a computer following Scheme I. For the sum $(k_{\text{fr}} + k_{\text{fi}} + k_{\text{r}})$, $\log(k, \text{s}^{-1}) = 15.6 - (13\,660/T)$; ^{20–22} k_{r} was set equal to $(k_{\text{fi}} + k_{\text{fr}})$, ignoring secondary deuterium kinetic isotope effects. For k_{g} , $\log(k, \text{s}^{-1}) = 13.6 - (14\,200/T)$.²³ Table I contains ratios of $k_{\text{fr}}/k_{\text{g}}$ and $k_{\text{fr}}/k_{\text{fi}}$ that best modeled the measured product ratios. Uncertainties are attributable to spectral noise and possible calibration errors in the TDL analyses. At 980 and 1048 K, other sources of error are comparatively negligible. At 1130 K, k_{r} , and thus $k_{\text{fr}}/k_{\text{g}}$, may be somewhat too large due to a competing channel for ethene production.

The $k_{\text{fr}}/k_{\text{g}}$ ratios of Table I show little temperature dependence over a 437-deg range in temperature. The $k_{\text{fr}}/k_{\text{fi}}$ ratios may be

- (5) Chickos, J. S. *J. Org. Chem.* **1979**, *44*, 780–784.
- (6) Dervan, P. B.; Santilli, D. S. *J. Am. Chem. Soc.* **1980**, *102*, 3863–3870.
- (7) Annamalai, A.; Keiderling, T. A.; Chickos, J. S. *J. Am. Chem. Soc.* **1984**, *106*, 6254–6262.
- (8) Chickos, J. S.; Annamalai, A.; Keiderling, T. A. *J. Am. Chem. Soc.* **1986**, *108*, 4398–4402.
- (9) Cannarsa, M. Ph. D. Thesis, Cornell University, 1984; Goldstein, M. J. Lecture, 8th IUPAC Conference on Physical Organic Chemistry, Tokyo, Japan, August 27, 1986.
- (10) Doubleday, C., Jr.; Camp, R. N.; King, H. F.; McIver, J. W., Jr.; Mullally, D.; Page, M. *J. Am. Chem. Soc.* **1984**, *106*, 447–448.
- (11) Bernardi, F.; Bottoni, A.; Tonachini, G.; Robb, M. A.; Schlegel, H. B. *Chem. Phys. Lett.* **1984**, *108*, 599–601. Bernardi, F.; Bottoni, A.; Robb, M. A.; Schlegel, H. B.; Tonachini, G. *J. Am. Chem. Soc.* **1985**, *107*, 2260–2264.
- (12) Chickos, J. S. *J. Org. Chem.* **1979**, *44*, 1515–1518.
- (13) Chickos, J. S.; Bausch, M.; Alul, R. *J. Org. Chem.* **1981**, *46*, 3559–3562.
- (14) Chickos, J. S. *J. Org. Chem.* **1986**, *51*, 553–558.
- (15) Lewis, D. K.; Giesler, S. E.; Brown, M. S. *Intern. J. Chem. Kinet.* **1978**, *10*, 277–294.

- (16) Lewis, D. K.; Greaney, M. A.; Sibert, E. L. *J. Phys. Chem.* **1981**, *85*, 1783–1786.
- (17) Lewis, D. K.; Cochran, J. C.; Hossenlopp, J.; Miller, D.; Sweeney, T. *J. Phys. Chem.* **1981**, *85*, 1787–1788.
- (18) Glenar, D. A.; Hill, A. *Rev. Sci. Instrum.* **1986**, *57*, 2493–2498.
- (19) Annamalai, A.; Keiderling, T. A. *J. Mol. Spectrosc.* **1985**, *109*, 46–59.
- (20) Barnard, J. A.; Cocks, A. T.; Lee, R. Y.-K. *J. Chem. Soc., Faraday Trans. 1* **1974**, *70*, 1782–1792.
- (21) Lewis, D. K.; Feinstein, S. A.; Jeffers, P. M. *J. Phys. Chem.* **1977**, *81*, 1877–1888.
- (22) Lewis, D. K.; Bergmann, J.; Mannoney, R.; Paddock, R.; Kalra, B. *K. J. Phys. Chem.* **1984**, *88*, 4112–4116.
- (23) As recommended by Benson, S. W. In *Thermochemical Kinetics*, 2nd ed.; Wiley-Interscience: New York, 1976; based on data of Douglas et al. (Douglas, J. E.; Rabinovitch, B. S.; Looney, F. S. *J. Chem. Phys.* **1955**, *23*, 315–323).

compared with the 1.3 value deduced by Dervan and Santilli⁶ at 712 K for tetramethylene derived from *cis*-3,4,5,6-TP-3,4-*d*₂. Others have found ratios of ethene-1,2-*d*₂ isomers from CB-1,2-*d*₂ at or near 1:1.^{5,9}

For an entropy-locked diradical, the data lead, via k_n/k_g ratios, to relative ΔG^\ddagger estimates for fragmentation versus ring closure of tetramethylene (Table I). The change in $\Delta\Delta G^\ddagger$ over the 693–1048 K range is negligible; the apparent increase in $\Delta\Delta G^\ddagger$ at 1130 °K may even be an artifact (see above).

Stereospecifically labeled substrates, shock tube techniques, and TDL analyses used in combination offer great promise in studies of the detailed thermal chemistry of simple hydrocarbons. Shock tube heating provides upward extension of temperatures, and avoids wall-catalyzed reactions. The TDL system eliminates spectral interferences; with planned system improvements, order of magnitude gains in precision should be realized. The present results, a preference for 3 from 1 and the absence of a significant temperature dependence for the k_t/k_g ratio, suggest either a very short lifetime for the diradical or a conservation-of-momentum effect as has been probed with the aid of trajectory calculations.²⁴

Acknowledgment. We thank the National Science Foundation for support of this work through Grant CHE-8419587 and the Research Corporation for a Cottrell College Science Grant (D.A.G.) and for a William and Flora Hewlett Foundation Grant (D.K.L.).

(24) Carpenter, B. K. *J. Am. Chem. Soc.* **1985**, *107*, 5730–5732.

Novel Three-Dimensional NMR Techniques for Studies of Peptides and Biological Macromolecules

C. Griesinger, O. W. Sørensen, and R. R. Ernst*

Laboratorium für Physikalische Chemie
Eidgenössische Technische Hochschule
8092 Zürich, Switzerland

Received June 30, 1987

Two-dimensional (2D) NMR¹ has succeeded to become the method of choice for the elucidation of biomolecular structure in solution.² The combination of J coupling correlation techniques, such as COSY and TOCSY, with cross-relaxation measurements, such as NOESY and ROESY, allows the determination of the three-dimensional structure of medium size proteins and nucleic acid fragments of molecular weight up to about 15 000.

Apart from possibly unfavorable relaxation times for large macromolecules, the molecular size limitation is primarily caused by spectral overlap in 2D frequency space. It is the purpose of this communication to demonstrate that the introduction of a third frequency dimension provides additional resolving power and exhibits considerable promise for future extensions of NMR structure elucidation methods.

Three-dimensional spectroscopy is a straightforward extension of 2D spectroscopy. The free induction decay is recorded as a function of the time variable t_3 with two independently incremented time parameters t_1 and t_2 . The three time periods are separated by two coherence transfer processes. The large set of $N_1 \times N_2$ experiments, where N_1 and N_2 are the sample numbers in t_1 and t_2 , respectively, necessarily leads to unacceptably long performance times when, for example, the full 10-ppm frequency range of protons were to be covered in all three dimensions. For this reason, we propose to limit sampling to restricted volumes of actual interest in 3D frequency space by application of frequency-selective pulses.

(1) Ernst, R. R.; Bodenhausen, G.; Wokaun, A. *Principles of NMR in One and Two Dimensions*; Clarendon Press: Oxford, 1987.

(2) Wüthrich, K. *NMR of Proteins and Nucleic Acids*; Wiley Interscience: New York, 1986.

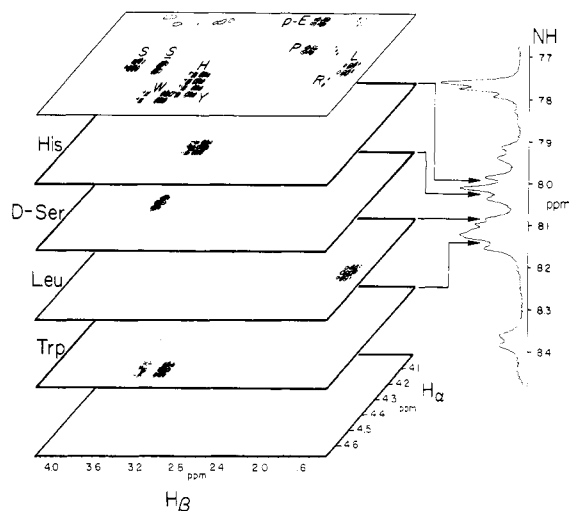


Figure 1. 3D COSY-COSY spectroscopy: On top is shown the $C_\alpha H$ - $C_\beta H$ cross-peak region of a 300-MHz soft-COSY experiment of 70 mM busserlin in $DMSO-d_6$. Four 2D cross sections of the 3D spectrum parallel to the $\omega_2(C_\alpha H)$ and $\omega_3(C_\beta H)$ axes are shown at NH frequencies of His, D-Ser, Leu, and Trp, respectively. The 3D data matrix of dimension $96 \times 96 \times 2048$ points, recorded in 48 h, was zero-filled to $256 \times 256 \times 4096$ points prior to the 3D Fourier transformation requiring 7 h on an ASPECT 1000 computer. The spectral width is $500 \times 500 \times 3000$ Hz. Contours are drawn for positive and negative intensities.

It is sufficient to apply selective excitation preceding the two evolution periods t_1 and t_2 . Nonselective pulses may precede the detection period, and selective detection in t_3 is only required in the case of limited data storage.

3D spectra can be obtained by various combinations of coherence transfer processes. In a COSY-COSY experiment, for example, both transfers involve the scalar J couplings (homonuclear and heteronuclear transfers can be arbitrarily combined³). In a NOESY-COSY experiment, on the other hand, the first transfer involves cross relaxation while the second is effected by J couplings. Combinations involving ROESY,^{4,5} TOCSY, multiple quantum excitation, or relayed transfer are also conceivable.

We demonstrate the features of 3D spectra by experiments on the linear nonapeptide busserlin, pyro-Glu-His-Trp-Ser-Tyr-D-Ser-Leu-Arg-Pro-NHCH₂CH₃ (p-E-H-W-S-Y-S-L-R-P-NHET). Figure 1 shows on top the moderately crowded $C_\alpha H$ - $C_\beta H$ cross-peak region of a 2D soft-COSY⁶ spectrum, obtained with the pulse sequence $(\pi/2)^{(C_\alpha H)}-t_1-(\pi/2)-t_2$ consisting of a selective and a nonselective pulse. The 3D COSY-COSY sequence with the pertinent coherence transfer $NH \rightarrow C_\alpha H \rightarrow C_\beta H$ leads to a 3D spectrum with $(\omega_1, \omega_2, \omega_3) = (\omega_{NH}, \omega_{C_\alpha H}, \omega_{C_\beta H})$. It requires the pulse sequence

$$(\pi/2)^{(NH)}-t_1-(\pi/2)^{(NH)}(\pi/2)^{(C_\alpha H)}-t_2-(\pi/2)-t_3$$

By displaying 2D cross sections of the 3D spectrum taken at fixed ω_1 frequencies, it is possible to spread the 2D $C_\alpha H$ - $C_\beta H$ cross-peak region according to the NH chemical shifts as is visualized in Figure 1. In this case each cross section contains only one cross peak that characterizes a particular amino acid residue by the three chemical shifts of NH, $C_\alpha H$, and $C_\beta H$ protons. The COSY-COSY experiment visualizes two-step relayed coherence transfer whereby the relay spin is uniquely identified in contrast to 2D relay experiments.⁷

(3) Griesinger, C.; Sørensen, O. W.; Ernst, R. R. *J. Magn. Reson.* **1987**, *73*, 574.

(4) Bothner-By, A. A.; Stephens, R. L.; Lee, J.; Warren, C. D.; Jeanloz, R. W. *J. Am. Chem. Soc.* **1984**, *106*, 811.

(5) Bax, A.; Davis, D. G. *J. Magn. Reson.* **1985**, *63*, 207.

(6) Brüschweiler, R.; Madsen, J. C.; Griesinger, C.; Sørensen, O. W.; Ernst, R. R. *J. Magn. Reson.* **1987**, *73*, 380.

(7) Eich, G. W.; Bodenhausen, G.; Ernst, R. R. *J. Am. Chem. Soc.* **1982**, *104*, 3731.